Programmable Pressure Pneumatic System for Soft Robots

Xinyu Xiao†, Kanghe Huang†, Renjie Zhu, Yahui Xue, Wenjin Wang,
Hongqiang Wang*, Jian S. Dai*, *Fellow, IEEE*

2023 IEEE International Conference on Robotics and Biomimetics (ROBIO) | 979-8-3503-2570-6/23/$31.00 ©2023 IEEE | DOI: 10.1109/ROBIO58561.2023.10354842

Abstract— **In the realm of soft robotics, the pneumatic system is a crucial component that plays an essential role in achieving optimal motion performance since all motion performance is ultimately linked to precise pressure control within the air chambers. To efficiently provide programmable pressure states for driving soft robots, this paper proposes a programmable pressure pneumatic system consisting of air pumps and valves with eight independent air channels. This system can provide precise hybrid negative and positive pressure for soft pneumatic robots. Closed-loop pressure control is achieved by sensing the pressure states in each air channel through sensors. Furthermore, two types of soft robots based on single-chamber soft pneumatic actuators are designed to verify the effectiveness and practicality of the pneumatic system. The proposed pneumatic system is a universal platform that can meet the pressure control requirements of various soft robots driven by both positive and negative pressure and holds significant implications for actuation and control in soft robotics.**

I. Introduction

Soft robotics is a critical branch of robotics, and pneumatic actuation is one of the primary methods used to drive soft robots.Compared to conventional rigid robots, soft robots have more degrees of freedom, flexibility, and enhanced environmental adaptability [1], [2], [3]. Soft pneumatic robots possess unique characteristics and advantages in design, manufacturing, and control, opening up new possibilities for advancing robotic technology [4], [5], [6].

Soft pneumatic robots utilize flexible materials and pneumatic drive systems, enabling them to adapt seamlessly to complex environments and tasks [7], [8]. These robots possess high deformation capacity, allowing for bending, stretching, and twisting actions that enable them to navigate irregular workspace and access hard-to-reach target positions [7], [9]. This inherent flexibility empowers soft pneumatic robots to perform intricate and versatile operations, including precise assembly within confined spaces, flexible manipulation, and rescue missions [2], [10].

Various driving methods exist for soft robots, such as pneumatic, hydraulic, and electroactive polymer driven systems [11]. Among these options, pneumatic driving stands out for its relative safety, convenience, and efficiency, making it widely employed in the realm of soft robotic. As for collaborative robotics, pneumatic fingers can effectively leverage the advantages of soft robotics and pneumatic systems to achieve end-effector force control.[12], [13]. For origami, pneumatic actuation holds great potential, some origami mechanisms exhibit variations in stiffness in different directions, which aligns well with the advantages of pneumatic actuation.[14], [15]. The driving system of soft pneumatic robots utilizes pumps as a power source, leveraging gas pressure and flow to control the expansion or bending of materials and thus control the robot's movements [16]. This pneumatic system boasts fast response times and exceptional controllability, allowing for precise position and force control [17], [18]. Consequently, soft robots find applications in various fields, including bio-inspired robotics, search and rescue operations, medical robotics, hydraulic/pneumatic systems, and artificial muscles [19], [20].

In general, soft pneumatic robots consist of three main components: a soft material actuating mechanism, solenoid valves forming the start-stop control system or pneumatic system, and air pumps serving as the driving devices.

The soft material actuating mechanism employs single or multiple chambers that undergo deformation by applying positive or negative pressure [4], [21]. Pneumatic actuators can be classified into three types: positive pressure-driven, negative pressure-driven, and hybrid pressure-driven [22]. The motion capabilities and performance of soft pneumatic robots are directly linked to the pressure conditions within the air chambers. By controlling the pressure state of multiple chambers, these robots can achieve various motions, such as bending, twisting, stretching, or contracting [23].

The pneumatic system serves as the driving mechanism for soft robots, given that the pressure state directly influences the motion performance of soft pneumatic robots within their chambers [24], [25], [26]. Therefore, it is crucial to have accurate pressure control to drive the soft actuators efficiently and effectively [27], [28].

To address this, we developed a programmable pressure system consisting of pumps and solenoid valves. This system comprises eight channels, each regulated by two solenoid valves that control the connection and cutoff of the positive and negative pressure pumps. Additionally, each channel is

*This work is supported in part by the National Natural Science Foundation of China under Grant 52275021, in part by the National Key R&D Program of China under Grant 2022YFB4701200, in part by the Science, Technology and Innovation Commission of Shenzhen Municipality under Grant ZDSYS20220527171403009, and in part by the Southern Marine Science and Engineering Guangdong Laboratory (Guangzhou), under Grant K19313901.

†These authors contributed equally to this work.

Xinyu Xiao, Kanghe Huang, Renjie Zhu, Jian S. Dai, and Hongqiang Wang are with Shenzhen Key Laboratory of Intelligent Robotics and Flexible Manufacturing Systems, Southern University of Science and Technology, Shenzhen, 518055, China.

Yahui Xue is with the Institute of Robotics, Southern University of Science and Technology, Shenzhen 518055, China.

Wenjin Wang is with the Institute of Robotics, Southern University of Science and Technology, Shenzhen 518055, China.

Jian S. Dai and Hongqiang Wang are the corresponding authors of this work. (email: daijs@sustech.edu.cn; wanghq6@sustech.edu.cn).

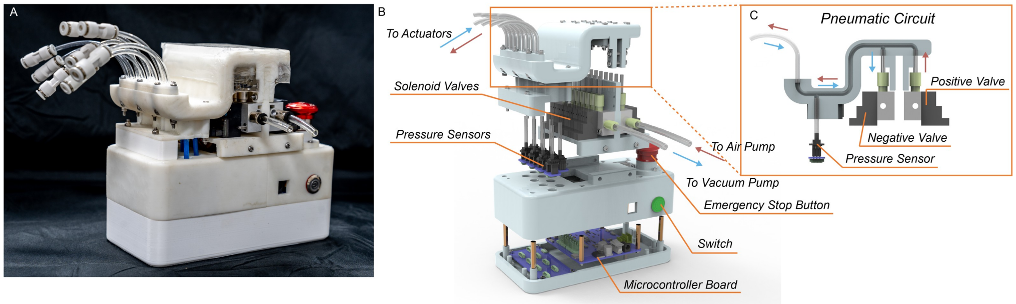

Fig. 1. Programmable pressure pneumatic system. (A) Prototype of the pneumatic system. (B) Explosion diagram of the pneumatic system. (C) Components Configuration of a single-channel pneumatic circuit.

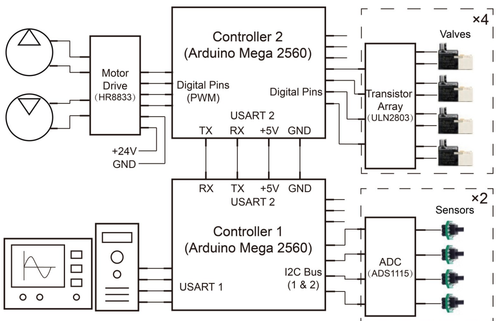

Fig. 2. Schematic diagram of the control circuit.

equipped with a pressure sensor to monitor the pressure within the circuit, enabling feedback control. With this setup, we can simultaneously control multiple chambers or implement sequential control. By controlling the pressure states of each air channel, we can precisely control the motion of the soft actuators.

II. Design of Pneumatic System

A. Structural configuration and pneumatic circuit

The motion performance of single-chamber soft robots depends on their internal pressure conditions, which can be categorized into three types: positive pressure-driven, negative pressure-driven, and hybrid pressure-driven. These classifications are the foundation for combining and creating more complex soft robots.

Here, to facilitate the efficient control of the soft actuators, a programmable hybrid-pressure pneumatic system is designed (Fig. 1A). The proposed pneumatic system consists of eight independent channels controlled by sixteen 2-way 2-state solenoid valves (H102-DL, Dighend), eight pressure sensors (XGZP6847A100KPGNPN, CFSensor), and an air pump (ED-0908, EidOLON) and a vacuum pump (750D, FUJIWARA) to generate positive and negative pressure, respectively (Fig. 1B). Each channel can serve as an inlet or outlet airflow, controlled by the positive and negative valves, according to the requirements. Additionally, the air pressure value in each channel is monitored by a pressure sensor (Fig. 1C).

B. Electrical circuit

The air pressure in the chambers of the soft actuators is primarily related to the air tightness of the chambers and pipelines, as well as the pressure feedback control. Due to the difficulty in achieving perfect air tightness in most soft robots' chambers, we developed a closed-loop pressure control system. By generating control signals using controllers and computers, the pressure in chambers can change as expected, allowing soft robots to perform corresponding movements.

As shown in Fig. 2, the control circuit consists of two controllers (Arduino Mega 2560) and peripheral circuits. Controller 1 is responsible for communicating with the computer, receiving control instructions from the computer, and transmitting them to Controller 2 to control solenoid valves. Additionally, it also feeds back the pressure signals measured by the sensors to the computer. The communication between two controllers is established through a serial port.

Furthermore, Controller 1 communicates with two 16-bit analog-to-digital converters (ADCs, ADS1115) through the I2C bus to read the pressure signals measured by eight pressure sensors. Controller 2 uses 16 digital pins to control the conduction of a transistor array (ULN2803), enabling all sixteen solenoid valves to open and close.

C. Strategies of pneumatic flow and closed-loop pressure control

The motion of soft robots can correspond to three pressure conditions inside their chambers: deflation, holding, and inflation, as well as combinations of these three basic pressure conditions. Based on the structural configuration, the closed-loop control strategy is proposed to control the pressure value. As shown in Fig. 3, during deflation, the negative valve is opened while the positive valve is closed, allowing air flows from the inner chamber of the actuator to the atmosphere environment through the operation of the vacuum pump. When the sensor detects that the pressure inside the soft robot chamber reaches the target pressure, both the negative and positive valves are closed, and the pneumatic system enters a holding state. If a target positive pressure command is given at this point, the positive valve is opened while the negative valve is closed, and the pneumatic

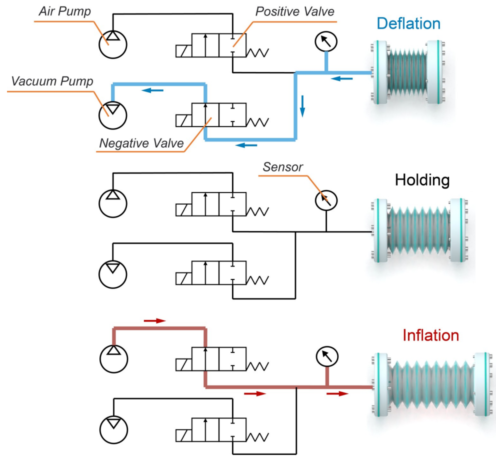

Fig. 3. Schematics and states of each component in deflation, holding, and inflation, respectively.

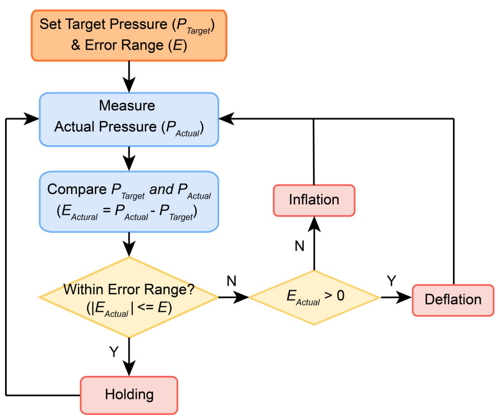

Fig. 4. Flowchart of closed-loop feedback pressure control strategy.

system starts to inflate the actuator until the sensor detects that the pressure has reached the target value.

Therefore, closed-loop feedback control can be achieved by monitoring the pressure measured by the pressure sensor, as shown in Fig. 4. Initially, the target pressure value (P_{Target}) and error range (E) of the actuator are set in advance. During each operation loop, the controller receives the current actual pressure value (P_{Actual}), compares it with the target pressure value (P_{Target}), and calculates the actual pressure error ($E_{Actual} = P_{Actual} - P_{Target}$).

If the error falls within the acceptable range, the system will enter a holding mode. However, if the error is beyond the acceptable range, the air pump and solenoid valve will be controlled based on the error. Specifically, if the error is positive, then deflation is executed, while if the error is negative, inflation is executed. By virtue of this loop process, the pneumatic system is able to achieve continuous pressure measurement and real-time closed-loop feedback.

III. Verification of the Pneumatic System

After completing the fabrication of the pneumatic system, we conducted a quantitative analysis and evaluation of its pressure characteristics. The pneumatic system consists of eight functionally identical pneumatic branches, each independently controllable. In the experiments, we tested a single pneumatic branch to illustrate the performance of the entire pneumatic system.

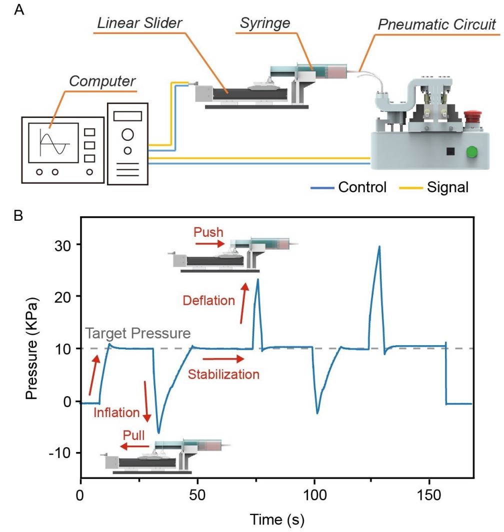

Fig. 5. Pressure response of the closed-loop pressure control experiment. (A) The schematic setup. (B) Experimental data for the experiment.

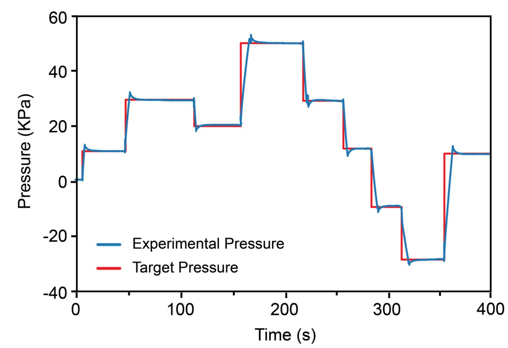

Fig. 6. Pressure step response of the pneumatic system.

A. Closed-loop pressure control

For soft robotics, closed-loop pressure control is crucial. The pneumatic system is required to maintain a stable pressure inside the actuator's chamber while also resisting disturbances caused by external environmental factors to achieve precise control of the soft actuators. This experiment is to test the pneumatic system's ability to maintain and stabilize air pressure through closed-loop pressure control.

As shown in Fig. 5A, the syringe is fixed on a platform, and its moving end is attached to the linear slider (LCE-5C-10-500-E, DH-Robotics). During the experiment, the syringe can be pushed or pulled by controlling the linear slider at a speed of 10 mm/s, thereby changing the volume of the syringe chamber. The other end of the syringe is connected to one of the branches of the pneumatic system, and the air pressure inside the syringe can be detected by activating the pressure sensor.

Initially, the syringe's cavity volume is fixed at 160 ml.

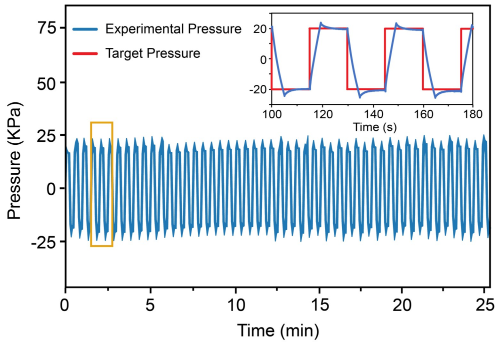

Fig. 7. Pressure response of the controllable positive and negative pressure cycling experiment.

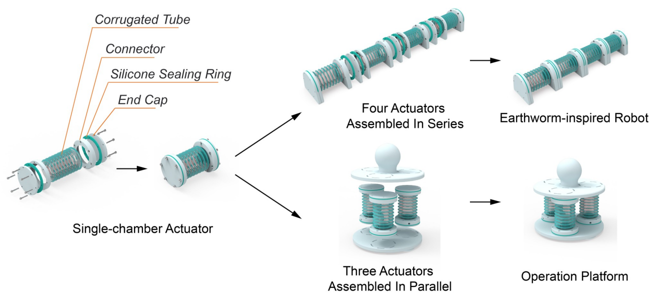

Fig. 8. An earthworm-inspired robot and an operation platform are designed by connecting single-chamber actuators in series and parallel, respectively.

The target pressure is set at 10 KPa (Fig. 5B). At the fifth second, the linear slider is controlled to pull the syringe outward, its cavity volume increases to 250 ml, and internal air pressure quickly drops below -7 KPa. At this point, the pressure sensor detects a deviation between the internal air pressure of the syringe and the target pressure, and the pneumatic system immediately opens the positive valve to inflate and adjust the internal pressure back to the target pressure (10 KPa). When the air pressure is stable, the error between the measured pressure and the target pressure is within 2 KPa.

Similarly, at the seventieth second, the slider is controlled to push the syringe inward, the internal air pressure of the syringe rapidly rises beyond 25 KPa, and the pneumatic system starts to deflate from the syringe, and the internal air pressure quickly returns to around 10 KPa.

During the experiment, we repeated this process twice to ensure the reliability of the results. As a result, the proposed pneumatic system is highly effective in maintaining the air pressure inside the actuator's chamber close to the target pressure and is capable of adjusting pressure back to the target level in response to pressure disturbances.

B. Step response of the pneumatic system

Figure 6 illustrates an experiment conducted to evaluate the performance of the proposed pneumatic system in response to sudden changes in the target pressure. The experiment is carried out with a fixed syringe volume of 500 ml, and the target pressure is abruptly changed from positive to negative and then back to positive. The positive pressure range is set between 0 and 50 KPa, while the negative pressure range is set between 0 and -30 KPa.

In summary, the system exhibits a high level of effectiveness in adjusting the air pressure to match the target pressure step changes, indicating its robustness and reliability in various operating conditions.

C. Controllable positive and negative pressure cycling

To verify the pneumatic system has the capability to switch freely between positive and negative pressure, we conducted the cycling experiment with a pressure range of -25 KPa to 25 KPa and a switching delay time of 15 s. The experiment is repeated 50 times to thoroughly evaluate the controllability and stability of the system under both positive and negative pressure states. As shown in Fig. 7, the pneumatic system can smoothly transition between positive and negative pressures while maintaining closed-loop pressure control throughout the process.

Based on the single-chamber testing experiment of the pneumatic system described above, the closed-loop control strategy proposed in our study can be extended to control the soft robots with multiple air chambers.

IV. Applications of the Pneumatic System

The programmable hybrid positive and negative pneumatic system proposed in this paper features a wide pressure range, which can be applied to soft robotic systems. Here, we designed soft actuators and robots to demonstrate practicality and convenience.

A. Single-chamber Soft Actuator

We designed a single-chamber soft actuator that can be connected to a pneumatic system to respond to positive and negative pressures with extension and contraction. As shown in Fig. 8, the actuator is composed of a corrugated tube sandwiched by 3D-printed connectors with silicone rings for sealing. The dimension of the actuator is 65 mm in length and 30 mm in diameter. Furthermore, the actuator as a basic unit can be assembled in series and parallel for different soft robotic applications.

Here, an earthworm-inspired robot is designed by connecting four single-chamber actuators in series using 3D-printed components. In addition to the parallel configuration, an operation platform is assembled by three single-chamber actuators equally spaced at 120° intervals on a circular path with a radius of 40 mm. Each actuator is connected to a branch of the pneumatic system and can be independently driven.

B. Earthworm-inspired Robot

Each soft segment of the earthworm-inspired robot is connected to an air circuit branch, as shown in Fig. 9. By controlling the timing of pressure states in the four segments, the robot can sequentially deflate and contract from the first to the fourth actuator unit for locomotion (Fig. 9A and B). The pressure range for each air circuit branch is

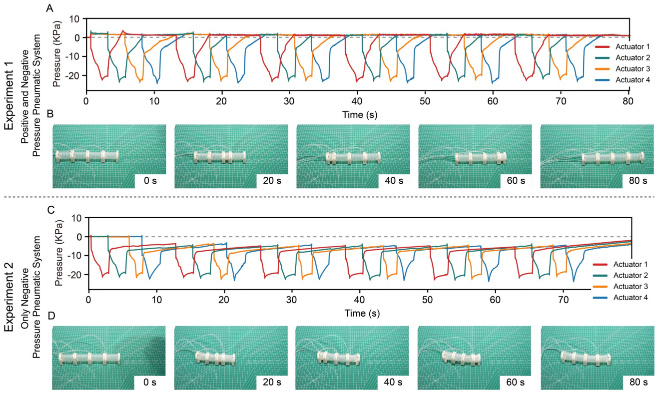

Fig. 9. The earthworm-inspired robot. (A) and (C) Pressure response of the earthworm-inspired robot. (B) and (D) The snapshots of the earthworm-inspired robot moving forward.

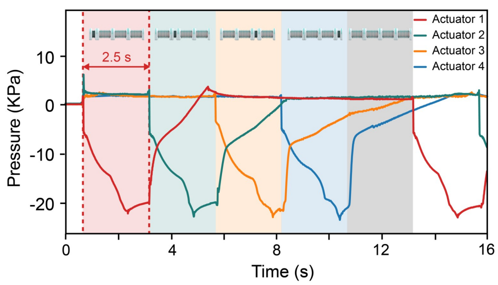

Fig. 10. Pressure response of the earthworm-inspired robot and its movement gait during one control cycle.

set from -20 KPa to 2 KPa. After six movement cycles, which take approximately 80 seconds, the earthworm-like robot moves forward approximately 160 mm. In Fig. 10, each soft segment of the earthworm-like robot deflates to -20 KPa and inflates to 2 KPa during one movement cycle. The first segment deflates initially, and after about 2.5 seconds, the second segment begins deflating as the first extends to 2 KPa, enabling a quick actuator rebound from compressed to extended. This repeats for subsequent segments until all four have deflated and inflated sequentially. One cycle takes approximately 12.5 seconds, and the robot proceeds to the next cycle. The step length, approximately 25 mm, depends on the difference between actuator extension and compression lengths.

We conducted two experiments to compare pneumatic systems: Experiment 1 utilized both positive and negative pressure pumps, while Experiment 2 relied solely on a negative pressure pump. In Experiment 1, the earthworm-like robot smoothly covered six step lengths (Fig. 9B). However, in Experiment 2, using only the negative pressure pump, the robot's motion was slow and deviated from the intended path (Fig. 9D). Experiment 1's positive pressure pump aided rapid inflation, allowing the actuator to rebound from -20 KPa to 2 KPa within 5 seconds (Fig. 9A). In contrast, Experiment 2 relied solely on pressure differential for inflation, significantly reducing the air volume entering the actuator's chamber. For example, it took nearly 10 seconds for the actuator's pressure to change from -20 KPa to -5 KPa (Fig. 9C). As a result, within the same 5-second cycle for inflation and deflation, the current actuator's inflation was incomplete when the next actuator's deflation started, causing instability in the earthworm-inspired robot's motion and deviation from its course.

In conclusion, compared to solely relying on the negative pressure pump and atmospheric pressure for inflation, a pneumatic system using both positive and negative pressure pumps is more effective and necessary.

C. *An operation platform based on the pressure recognition*

As shown in Fig. 8, an operation platform is created by connecting three single-chamber actuators in parallel. By simultaneously controlling the pressure state of different chambers, the platform's motion can be achieved. When the valves are closed, the internal pressure in the chambers change with the volume, which can be used to identify the platform's motion by measuring the changes in the pressure of three chambers.

The base of the parallel operation platform is fixed on the desktop, and the positions of the three actuators are distributed, as shown in Fig. 11. Each actuator is independently connected to the pneumatic system, and both positive and negative valves are closed to maintain a constant chamber volume. The platform can perform movements such as elongation and compression along the Z-axis and bending around the X-axis and Y-axis.

For practical use, we employed a parallel platform in Unity to control a humanoid character's movements. The platform's motion triggers pressure changes in three chambers, which correspond to the character's actions (such as walking, turning, and jumping). For instance, when a vertical force is applied to the platform, the volume of these chambers decreases simultaneously, causing the pressure to rise to 15 KPa. At this point, the pressure levels in the three chambers serve as a signal for the humanoid character to jump. Similarly, bending the platform to the left around the X-axis controls the virtual character's left turn. Chamber 2 is compressed, increasing air pressure, while Chamber 1 is stretched, resulting in decreased air pressure, with Chamber 3 experiencing minimal change. Conversely, when the air pressure in Chamber 2 and Chamber 1 is reversed, the platform bends to the right around the X-axis, causing the virtual character to turn right. Additionally, we define platform bending in two directions around the Y-axis as the virtual character moving forward and executing a 180-degree turn.

In summary, by correspondingly controlling the parallel platform with the pressure states of the three air chambers, we achieve good control results for the motion of the virtual character.

V. Conclusion

In this paper, we proposed a pneumatic system capable of providing programmable pressure states for soft robots to meet various pressure requirements. The system employs positive and negative pressure pumps as pressure sources,

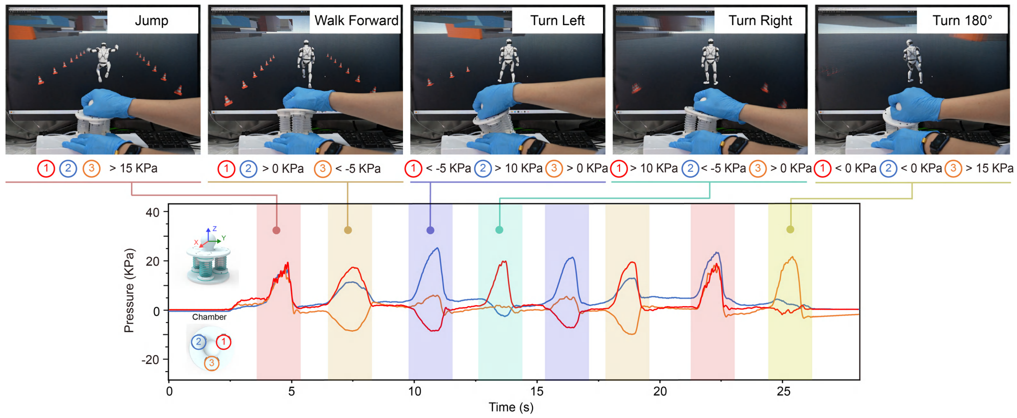

Fig. 11. The VR application of the operation platform with three single-chamber actuators for the Robot's motion control according to the chamber pressure recognition.

with controlled inflation and deflation achieved by controlling the on-off states of solenoid valves. Additionally, closed-loop pressure control is designed to attain precise control of the pressure states. The system has eight independent air channels that can be controlled separately, providing a wide pressure scale ranging from negative to positive pressure states that are accurate and stable.

To further validate the practicality of the developed pneumatic system, we designed a single-chamber soft actuator, earthworm-inspired robot, and parallel operation platform and tested their performance through experiments. The results demonstrate that the pneumatic system can meet the driving requirements of most soft pneumatic robots and can serve as a universal pneumatic platform, making it highly practical for actuating soft robots.

REFERENCES

[1] N. Elango and A. A. M. Faudzi, "A review article: investigations on soft materials for soft robot manipulations," Int. J. Adv. Manuf. Technol., vol. 80, pp. 1027–1037, 2015.

[2] D. Li, et al., "Origami-inspired soft twisting actuator," Soft Robot., vol. 10, no. 2, pp. 395-409, 2023.

[3] J. S. Dai, N. Holland, and D. R. Kerr, "Finite twist mapping and its application to planar serial manipulators with revolute joints," Journal of Mechanical Engineering Science, vol. 209, no. 4, pp. 263–271, 1995.

[4] D. Fan, et al., "Innervation of Sensing Microchannels for Three-Dimensional Stimuli Perception," Adv. Mater. Technol., p. 2300185, 2023.

[5] R. Zhu, et al., "Soft Robots for Cluttered Environments Based on Origami Anisotropic Stiffness Structure (OASS) Inspired by Desert Iguana," Adv. Intell. Syst., vol. 5, no. 6, p. 2200301, 2023.

[6] D. Fan, et al., "Self-shrinking soft demoulding for complex high-aspect-ratio microchannels," Nat. Commun., vol. 13, no. 1, p. 5083, 2022.

[7] E. W. Hawkes, et al., "A soft robot that navigates its environment through growth," Sci. Robot., vol. 2, no. 8, 2017, eaan3028.

[8] Q. Xiong, et al., "Earthworm-Inspired Multi-Material, Adaptive Strain-Limiting, Hybrid Actuators for Soft Robots," Adv. Intell. Syst., vol. 5, no. 3, p. 2200346, 2023.

[9] S. Hoang, et al., "A pneumatic random-access memory for controlling soft robots," PLOS ONE, vol. 16, no. 7, 2021, e0254524.

[10] J. Guo, et al., "Design and fabrication of a pneumatic soft robotic gripper for delicate surgical manipulation," in 2017 IEEE International Conference on Mechatronics and Automation (ICMA), IEEE, pp. 1069-1074, 2017.

[11] C. Lee, et al., "Soft robot review," Int. J. Control Autom. Syst., vol. 15, pp. 3-15, 2017.

[12] A. Ghafoor, J. S. Dai, and J. Duffy, "Stiffness modeling of the soft-finger contact in robotic grasping," Journal of Mechanical Design, vol. 126, pp. 646–656, 2004.

[13] H. Liu and J. S. Dai, "An approach to carton-folding trajectory planning using dual robotic fingers," Robotics and Autonomous Systems, vol. 42, no. 1, pp. 47–63, 2003.

[14] J. Zhao, et al., "Structure synthesis and statics analysis of a foldable stair," Mechanism and Machine Theory, vol. 46, no. 7, pp. 998–1015, 2011.

[15] J. S. Dai and D. G. Caldwell, "Origami-based robotic paper-and-board packaging for food industry," Trends in Food Science and Technology, vol. 21, no. 3, pp. 153–157, 2010.

[16] Y. Li, et al., "Precharged pneumatic soft actuators and their applications to untethered soft robots," Soft Robotics, vol. 5, no. 5, pp. 567-575, 2018.

[17] R. J. Sanchez, et al., "A pneumatic robot for re-training arm movement after stroke: Rationale and mechanical design," in 9th International Conference on Rehabilitation Robotics (ICORR), IEEE, pp. 500-504, 2005.

[18] D. Sasaki, T. Noritsugu, and M. Takaiwa, "Development of pneumatic soft robot hand for human friendly robot," J. Robot. Mechatron., vol. 15, no. 2, pp. 164-171, 2003.

[19] R. B. N. Scharff, et al., "Sensing and reconstruction of 3-D deformation on pneumatic soft robots," IEEE/ASME Trans. Mechatronics, vol. 26, no. 4, pp. 1877-1885, 2021.

[20] R. F. Shepherd, et al., "Multigait soft robot," Proc. Natl. Acad. Sci., vol. 108, no. 51, pp. 20400-20403, 2011.

[21] D. Fan, et al., "Flow Casting Soft Shells with Geometrical Complexity and Multifunctionality," Adv. Mater. Technol., vol. 8, no. 8, p. 2201640, 2023.

[22] H. Su, et al., "Pneumatic soft robots: Challenges and benefits," Actuators, vol. 11, no. 3, p. 92, 2022.

[23] E. Todorov, et al., "Identification and control of a pneumatic robot," in Proceedings of the 2010 IEEE International Conference on Biomedical Robotics and Biomechatronics (BioRob), pp. 373-380, 2010.

[24] J. Walker, et al., "Soft robotics: A review of recent developments of pneumatic soft actuators," Actuators, vol. 9, no. 1, p. 3, 2020.

[25] R. Hashem, et al., "Design and characterization of a bellows-driven soft pneumatic actuator," IEEE/ASME Transactions on Mechatronics, vol. 26, no. 5, pp. 2327-2338, 2020.

[26] S. Lee, D. Lee, and D. Shin, "An air recirculation system based on bioinspired soft re-air valve for highly efficient pneumatic actuation," Soft Robotics, vol. 8, pp. 564-576, 2021.

[27] B. Zhang, et al.,"Pneumatic system capable of supplying programmable pressure states for soft robots," Soft Robotics, vol. 9, no. 5, pp. 1001-1013, 2022.

[28] S. Joshi and J. Paik, "Pneumatic supply system parameter optimization for soft actuators," Soft Robotics, vol. 8, pp. 152-163, 2021.